Dependence of the density limit on the toroidal magnetic field on FTU

2013 Nucl. Fusion 53 023007

(http://iopscience.iop.org/0029-5515/53/2/023007)

IOP Publishing and International Atomic Energy Agency Nuclear Fusion
Nucl. Fusion **53** (2013) 023007 (7pp) doi:10.1088/0029-5515/53/2/023007

Dependence of the density limit on the toroidal magnetic field on FTU

G. Pucella[1], O. Tudisco[1], M.L. Apicella[1], G. Apruzzese[1], G. Artaserse[1], F. Belli[1], W. Bin[2], L. Boncagni[1], A. Botrugno[1], P. Buratti[1], G. Calabrò[1], C. Castaldo[1], C. Cianfarani[1], V. Cocilovo[1], L. Dimatteo[1], B. Esposito[1], D. Frigione[1], L. Gabellieri[1], E. Giovannozzi[1], G. Granucci[2], M. Marinucci[1], D. Marocco[1], E. Martines[3], G. Mazzitelli[1], C. Mazzotta[1], S. Nowak[2], G. Ramogida[1], A. Romano[1], A.A. Tuccillo[1], L. Zeng[4] and M. Zuin[3]

[1] C.R. ENEA, Assoc. Euratom-ENEA, Via E. Fermi 45, I-00044 Frascati, Italy
[2] IFP-CNR, Assoc. Euratom-ENEA, Via R. Cozzi 53, I-20125 Milano, Italy
[3] Consorzio RFX, Assoc. Euratom-ENEA, Corso Stati Uniti 4, I-35127 Padova, Italy
[4] Institute of Plasma Phys., Chinese Academy of Sciences, Hefei, 230031, People's Republic of China

E-mail: gianluca.pucella@enea.it

Received 27 April 2012, accepted for publication 7 January 2013
Published 1 February 2013
Online at stacks.iop.org/NF/53/023007

Abstract
The capability of predicting the density limit of a magnetically confined burning plasma is of crucial importance to establish the ultimate performance of a fusion power plant. The Greenwald density limit, commonly used as an empirical scaling law, predicts that the maximum achievable central line-averaged density is given by the relation $\bar{n}_G = k\bar{J}$, where $\bar{J}$ is the average plasma current density and k is the plasma elongation. However, several experiments have pointed out that such a limit can be overcome in the presence of peaked density profiles. This paper proposes a new empirical scaling law for a limiter tokamak operating in the low-energy confinement mode (L-mode) concerning the case of peaked density profiles associated with the presence of multifaceted asymmetric radiation from the edges. This result is based on dedicated experiments performed on the Frascati Tokamak Upgrade (FTU) under extremely clean machine conditions ($Z_{eff} = 1.0$–1.5), in which the high-density domain is explored in a wide range of values of plasma current ($I_p = 500$–900 kA) and toroidal magnetic field ($B_T = 4$–8 T). It is found that the maximum achievable central line-averaged density essentially depends on the toroidal magnetic field only and does not depend on the average plasma current density: the behaviour is explained in terms of density profile peaking in the high-density domain. As a confirmation that the limit is an edge limit, it is also shown that a Greenwald-like scaling (i.e. depending on the current density) actually holds for the edge line-averaged density (at $r/a \simeq 4/5$).

(Some figures may appear in colour only in the online journal)

1. Introduction

A severe problem in fusion research concerns the density to be used in fusion devices, as in order to obtain large efficiencies in a fusion power plant it is mandatory to have long energy confinement times (related to the power losses) with high plasma density [1]. For this reason, in tokamak fusion devices (in which a plasma is magnetically confined in a toroidal configuration) it is of great interest to operate at high density and a large amount of effort has been devoted to increase the plasma density, which is observed to be limited by the appearance of catastrophic events, so-called 'disruptions', causing loss of plasma confinement. An important role in the disruptions for density limit is played by magnetohydrodynamic (MHD) instabilities associated with the steepening of the current density profile due to a current channel shrinkage [2, 3]. In this picture the contraction of the current channel with increasing densities is related to the plasma edge cooling induced by an influx of strongly radiating light impurities desorbed from the torus walls. This suggests that the disruption can be avoided if the heating is sufficient to prevent the plasma edge cooling and we may expect that by increasing the ohmic heating power input the plasma density limit will increase. In 1988 Greenwald *et al* [4], by

bringing together data from many ohmically heated tokamak experiments, showed that the maximum achievable central line-averaged density (expressed in units of 10^{20} particles m^{-3}) is given by the relation $\bar{n}_G = k\bar{J}$, where $\bar{J}$ is the average plasma current density (expressed in units of MA m^{-2}) and k is the plasma elongation. In particular, for elliptical cross sections the previous scaling law for the density limit can be written as $\bar{n}_G = I_p/\pi a^2$, where I_p (in MA) is the plasma current and a (in m) is the minor radius of the ellipse. Now, if we introduce, for a circular plasma, the cylindrical edge safety factor q_{cyl}, we can write $q_{cyl}^{-1} = (\pi/5)(I_p/\pi a^2)/(B_T/R)$ and we see that the inverse edge safety factor is proportional to the average plasma current density, with a normalization factor given by the ratio between the toroidal magnetic field (B_T) and the plasma major radius (R). The plot of the 'normalized average current' q_{cyl}^{-1} versus the 'normalized average density' $\bar{n}/(B_T/R)$ (the so-called *Murakami number*) is usually referred to as the *Hugill plot* and in this plot the *Greenwald density limit* $\bar{n}_G$, which is currently the most used one, corresponds to a straight line with slope $\pi/5$. It is worth noting that the Greenwald density limit has been exceeded in tokamak experiments, but usually in the case of peaked density profiles (due to core fuelling, edge pumping, pellet injection, particle transport modification, etc) [5–8], indicating that the edge density is the real parameter responsible for the density limit [9]. Recently, it has been shown on the Frascati Tokamak Upgrade (FTU) [10] that, for a given plasma current, the Greenwald density limit can be exceeded in gas-fuelled discharges with a high value of the edge safety factor [11, 12], thus suggesting a possible dependence of the density limit on the toroidal magnetic field. The aim of this paper is to present the results of dedicated density limit experiments performed on FTU confirming the edge nature of the density limit and suggesting a new formulation of the density limit scaling law, based on a dependence on B_T only, for ohmically heated, gas fuelled, limited plasma discharges in L-mode in the presence of the MARFE (multifaceted asymmetric radiation from the edge) phenomenon. There is an extensive literature on experimental and theoretical studies of the density limit and of the MARFE (see [9, 13] for comprehensive reviews). Here, we will mention only the papers that are relevant to this work, to compare the FTU results with those from other devices.

2. Experimental set-up

FTU is a compact high magnetic field machine (B_T ranging from ~2.5 up to 8 T) with I_p up to 1.6 MA, circular poloidal cross-section (plasma major radius $R = 0.935$ m, plasma minor radius $a = 0.28$ m) and metallic first walls. The stainless steel vacuum chamber has a thickness of 2 mm and a radius of 0.33 m and is covered internally by a toroidal limiter made of 2 cm thick molybdenum tiles. In order to reduce the oxygen content, FTU walls are conditioned with boron coating at the beginning of any experimental campaign. The plasma position is controlled by a real-time feedback control system and the gas puffing into the plasma is managed by means of piezoelectric valves. The electron density is measured by a high-resolution CO_2/CO scanning interferometer along more than 30 vertical chords [14]; in particular, the central line-averaged density $\bar{n}_0$ reported in this work refers to the vertical chord passing through the magnetic axis, localized at $R_M = 0.95$ m, while the reconstructed density profiles are obtained by an inversion procedure starting from the line-averaged densities of the different chords [11]. The radiation losses are measured by a bolometer array, while D_α (for a deuterium plasma) and bremsstrahlung emissions are measured through two different collection optics along horizontal and vertical chords, respectively, and the average value of the ion effective charge Z_{eff} is derived from the bremsstrahlung data using the experimental electron density and temperature profiles.

At high-density operation, an increase in the density beyond a certain value usually produces the MARFE phenomenon [13] before reaching the density limit [11, 12]. The term 'MARFE' defines a radiative thermal instability of the edge plasma characterized by a toroidally symmetric and poloidally asymmetric belt of high density, strongly radiating, cold plasma localized at the high-field side of the tokamak, with short poloidal and radial extent. When the MARFE appears, the visible light camera shows a toroidal ring of strong D_α emission from this zone. After the MARFE onset, with increasing density the small ring observed by the camera expands poloidally and when the MARFE is well developed its motion results in strong and fast oscillations observed on the CO_2/CO interferometer, starting from the high-field side chords. This is why particular care is taken in the reconstruction of the density profile in the presence of a MARFE [11].

3. Results and discussion

We explored the high-density domain in a wide range of values of I_p and B_T to investigate a possible dependence of the density limit on B_T. For this work we considered three different values for the plasma current (I_p = 500, 700, 900 kA) and for each of them we considered five different values for the toroidal magnetic field (B_T = 4.0, 5.2, 6.0, 7.2, 8.0 T). For each (I_p, B_T) configuration we performed a discharge where a continuous gas flow was injected into the plasma to produce an increasing density up to the disruption for the density limit, occurring due to the rapid increase in the amplitude of MHD activity (the only selection criterion for these discharges being the density limit to be reached during the I_p flat-top). All discharges considered here had gas puffing and ohmic heating only and were performed under extremely clean machine conditions (typically Z_{eff} = 1.0–1.5).

In figure 1 the time traces of some relevant quantities are reported for a specific discharge with $I_p = 700$ kA and $B_T = 7.2$ T: (*a*) D_α emission, (*b*) temperature at $r/a = 0, 0.8$, (*c*) line-averaged density at $r/a = 0, 0.8$, (*d*) peaking factor of the density profile (obtained as the ratio $n(0)/\langle n\rangle$ between the central density and the volume-averaged density), (*e*) energy confinement time, (*f*) total particle number injected from all the valves. As we can see, at $t = 0.5$ s the D_α emission starts to rise as a consequence of the MARFE formation: this typically occurs when the edge temperature drops to a few eV as the density ramps up. Afterwards, there is a peaking of the density profile, as evidenced by the progressive increase seen on the central chord of the interferometer, while the value of the peripheral chord remains almost unchanged. In particular, the density peaking has a good effect on the energy

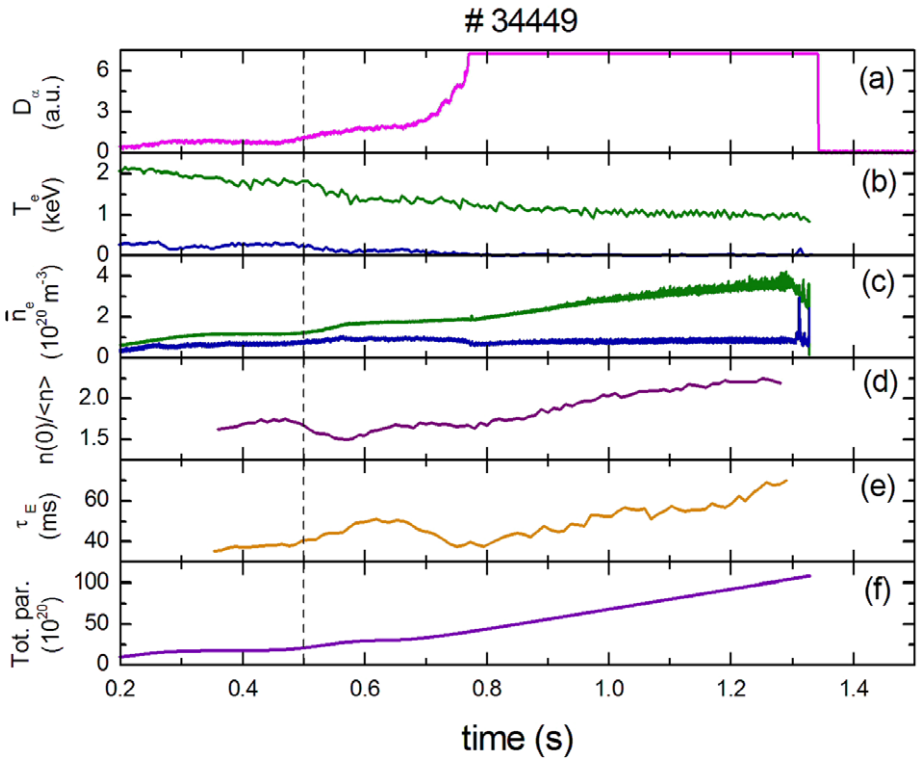

Figure 1. Time traces of some relevant quantities for a specific discharge with $I_p = 700\,\text{kA}$ and $B_T = 7.2\,\text{T}$: (*a*) D_α emission, (*b*) temperature at $r/a = 0, 0.8$, (*c*) line-averaged density at $r/a = 0, 0.8$, (*d*) peaking factor of the density profile, (*e*) energy confinement time, (*f*) total particle number injected from all the valves.

confinement time [12] (as evaluated by means of the transport code JETTO [15]), which increases to higher values (up to 70 ms) as the density peaking overcomes a threshold value of about 1.7. Finally, we report that the loop voltage increases from 2.0 to 2.3 V in the period corresponding to the increase in the density peaking.

It is worth noting that strongly peaked density profiles, with a peaking factor above 2, can be sustained for many energy confinement times. As an example, in figure 2 the time traces of the central and peripheral line-averaged density, the peaking factor of the density profile, and the total particle number injected into the tokamak are reported for a specific discharge with $I_p = 500\,\text{kA}$ and $B_T = 7.2\,\text{T}$. In this discharge the gas flow was managed to obtain a density plateau at a density value of 3.4×10^{20} particles m^{-3}, slightly below the density limit of 3.9×10^{20} particles m^{-3} obtained for the same values of I_p and B_T. The current flat-top was terminated at $t = 1.4\,\text{s}$ and the disruption occurred during current ramp-down at $I_p = 110\,\text{kA}$. As we can see, in such a case FTU has been able to operate at a central line-averaged density well above the value $\bar{n}_G = 2.0 \times 10^{20}$ particles m^{-3} expected from the Greenwald scaling law, thanks to the high value of the peaking factor, which remains above 2.5 for about 400 ms, namely seven times the value of the energy confinement time obtained for this discharge. In particular, we can observe that after $t = 1.2\,\text{s}$ the gas puff of the real-time feedback control system is no longer necessary to maintain the central line-averaged density above the programmed value, because in the high-density regime on FTU the plasma density is sustained by the high recycling fluxes. In this discharge with very high density a stationary value was not achieved for the density peaking, probably due to the limitation of duration of the discharge and the need to have a density ramp not very steep. Nevertheless, if we consider discharges at lower densities (see figure 3), a constant value of the central line-averaged density can be sustained for a longer time, with a specific value of the peaking factor, confirming that the density peaking is not a transient phenomenon, at least at these lower densities. It is worth noting that while in the high-density regime on FTU ($\bar{n}_0 > 1.5 \times 10^{20}$ particles m^{-3}) the plasma density is sustained in a stationary, but not controlled, way by the high recycling fluxes, in the low and intermediate density regime ($\bar{n}_0 < 1.5 \times 10^{20}$ particles m^{-3}) a stationary plasma density can be sustained in a controlled way by adjusting the gas puff, also in the presence of a well-developed MARFE [11, 12].

Coming back to line-averaged densities, figure 4(*a*) shows the Hugill plot of the complete dataset. For each discharge, the parameters corresponding to the onset of the MARFE, as identified from the rise of the D_α emission (open symbols), and to the disruption for density limit (solid symbols) are reported on the plot, and the Greenwald density limit is marked by a solid line. As we can see from the figure, the central line-averaged density corresponding to the onset of the MARFE is a linear function of the plasma current density (dashed line in the plot), substantially independently of B_T, and this is in agreement with the usually observed scaling [13, 16]; in particular, the MARFE occurs on FTU at 40% of the Greenwald limit (some machines report the onset of the MARFE much closer to the Greenwald limit). Different behaviour is observed for the density limit, that is not scaling linearly with the plasma current density; in particular, it is clear from figure 4(*a*) that the Greenwald limit

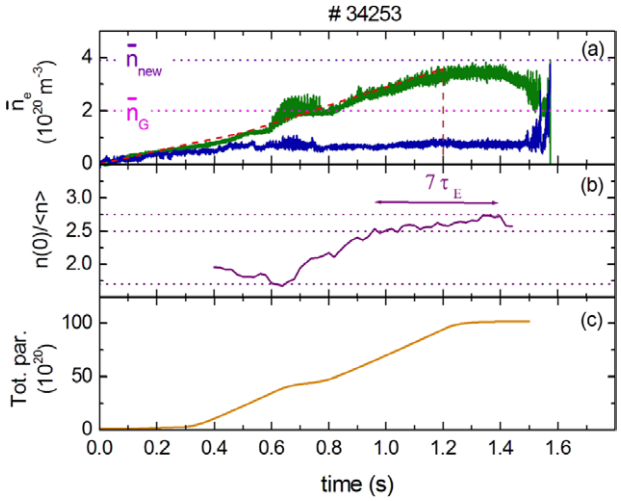

Figure 2. Time traces of some relevant quantities for a specific discharge with $I_p = 500$ kA and $B_T = 7.2$ T: (*a*) line-averaged density at $r/a = 0, 0.8$, (*b*) peaking factor of density profile, (*c*) total particle number injected from all the valves. The dotted lines reported in (*a*) correspond to the maximum achievable central line-averaged density as expected from the Greenwald scaling law and as obtained on FTU in a similar discharge, while the dashed line corresponds to the pre-programmed central line-averaged density.

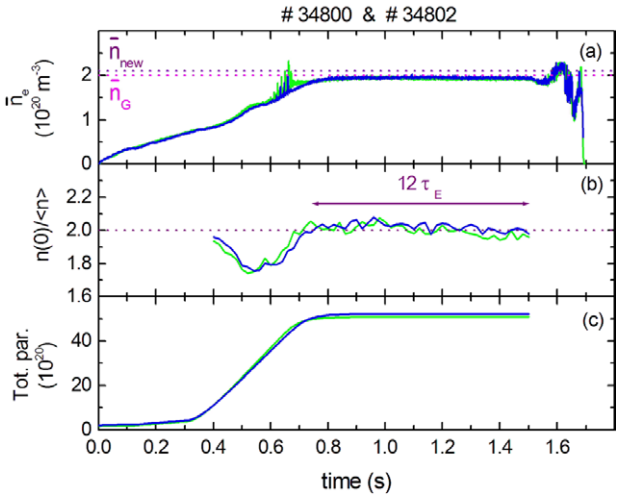

Figure 3. Time traces of some relevant quantities for two specific discharges with $I_p = 500$ kA and $B_T = 5.2$ T: (*a*) central line-averaged density, (*b*) peaking factor of density profile, (*c*) total particle number injected from all the valves. The dotted lines reported on (*a*) correspond to the maximum achievable central line-averaged density as expected from the Greenwald scaling law and as obtained on FTU in a similar discharge.

is exceeded for discharges with a high value of q_{cyl}, while it is not reached for discharges with a low value of q_{cyl}.

From a closer inspection of the data, it turns out that the density peaking is approximately constant at the onset of the MARFE, ranging between 1.3 and 1.7, as shown in figure 5 (open symbols), where the values of the density peaking are reported as a function of the value of q_{cyl} for different B_T and I_p. However, after the onset of the MARFE, with increasing density there is a spontaneous peaking of the density profiles which depends on I_p and B_T. For example, for a fixed B_T, the density profiles at higher I_p are systematically broader than those at low I_p, while, for a fixed I_p, the density profiles at lower B_T are systematically broader than those at high B_T. Therefore, a strong peaking of the density profiles is observed on FTU for low I_p and/or for high B_T associated with the presence of a MARFE. In particular, in our data the values of the density peaking at the disruption for the density limit strongly depend on q_{cyl}, as shown in figure 5 (solid symbols) and then for the same edge line-averaged density the central line-averaged density at the disruption is higher for higher values of q_{cyl}. This behaviour can help explain the reason why the Greenwald density limit is exceeded in our data for high values of q_{cyl} (as shown in figure 4(*a*)) and suggests that the edge line-averaged density, instead of the central one, may be the actual limiting parameter resulting from the power balance between the heating power input and the radiative losses associated with the light impurities desorbed from the torus walls. In fact, in many tokamaks there is strong evidence linking the density limit to the physics near the plasma boundary and the Greenwald density limit has been extended in several experiments increasing the central density at constant edge density. Using high-speed pellet injection on FTU, ASDEX and JT-60 [7, 17, 18], the limit has been extended considerably, as the plasma is fuelled directly at the centre with an evident increase in the density peaking. Similar effects have been obtained on DIII-D, DITE and ASDEX with NBI heating and strong edge pumping [8, 17, 19, 20] to reduce plasma recycling. Steady-state discharges with peaked density profiles are also obtained on TEXTOR and HT-7 by injecting impurity at the edge [21–23], e.g. by neon puffing, which creates a mantle of cold radiating plasma. In all the experiments cited here, the edge density stayed below the empirical density limits and the increase in the central line-averaged density came from particles in the plasma core, in agreement with models which attribute the density limit to physics in the plasma edge. We therefore present in figure 4(*b*) a '*modified* Hugill plot' of the complete dataset considering, instead of the central line-averaged density $\bar{n}_0$, the edge line-averaged density $\bar{n}_{4/5}$ referring to the vertical chord passing through the external part of the plasma column (at $r/a \simeq 4/5$). As we can see from figures 4(*a*) and (*b*), both the edge and central line-averaged density values corresponding to the onset of the MARFE are linear functions of the plasma current density (see the dashed lines). In contrast, only the edge line-averaged density value corresponding to the disruption for the density limit scales linearly with the plasma current density, while this does not occur with the central line-averaged density at the disruption (see the solid lines): such a result confirms that, indeed, the edge density is the real limiting parameter responsible for the density limit [9] and therefore we can define an '*edge Greenwald limit*', $\bar{n}_{G_{edge}} \simeq 0.36 \times (I_p/\pi a^2)$, as indicated by the solid line in figure 4(*b*). On the other hand, when the central line-averaged density is considered, the density profile effect plays a crucial role in the determination of the scaling law corresponding to the density limit.

In the discharges considered here, the density profile starts peaking just after the MARFE appearance, hence the mechanism of the peaking should be sought in the MARFE properties. The MARFE instability is caused by a reduction in the parallel thermal conductivity at the edge as the plasma edge temperature decreases with increasing density. Under such conditions a local cold and dense plasma blob, the MARFE,

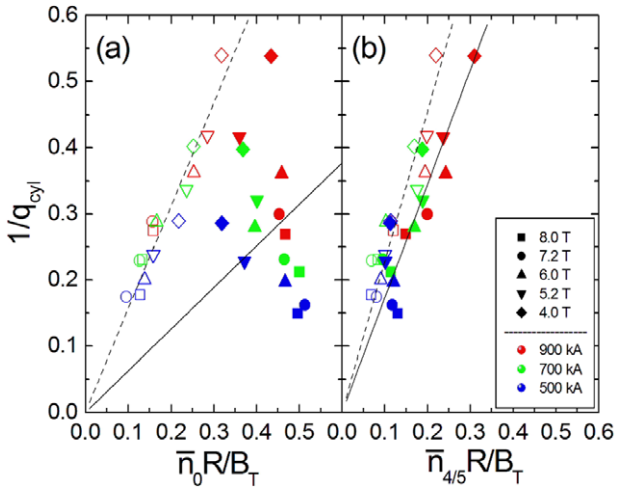

Figure 4. (*a*) Hugill plot of the FTU discharges. Open symbols refer to the onset of the MARFE and solid symbols refer to the disruption for density limit. Different symbols are used for different B_T and different colours are used for different I_p (see box in the figure). The solid line corresponds to the Greenwald density limit $\bar{n}_G$, while the dashed line corresponds to a fraction of $\bar{n}_G$. (*b*) Modified Hugill plot of the FTU discharges: edge line-averaged densities $\bar{n}_{4/5}$ (at $r/a \simeq 4/5$) are used instead of the central line-averaged densities $\bar{n}_0$. The solid and dashed lines correspond to different fractions of $\bar{n}_G$.

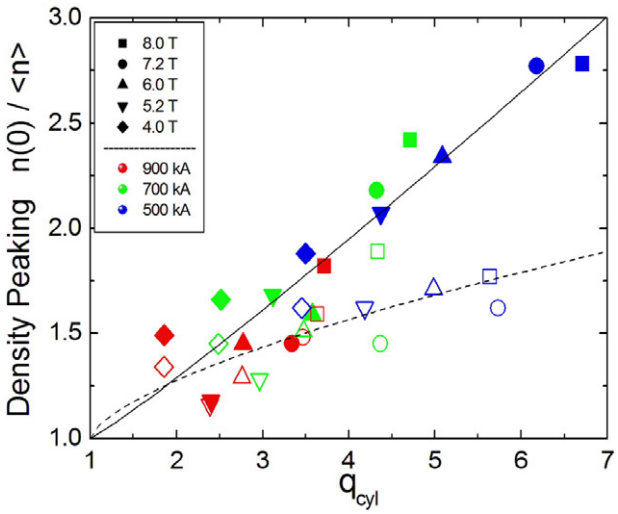

Figure 5. Density peaking at the onset of the MARFE (open symbols) and at the disruption for density limit (solid symbols) as a function of q_{cyl}, for discharges with different B_T and I_p (see the box in the figure for the meaning of symbols and colours). The lines reported on the plot are only a guide to the eye.

can form where the thermal flux is lower (usually in the high-field side of the poloidal section). Experimentally, a sharp rise in the D_α emission is observed, immediately followed by a temperature drop in a thick layer at the edge ($4/5 < r/a < 1$): only after this temperature drop does the density profile start peaking [11]. The enhanced D_α emission inside the MARFE, which is located inside the last closed surface, is an indication that the neutral particles are penetrating deeply inside the plasma. Practically, in this heuristic model, the MARFE is a short-cut for neutral particles to access the good confinement region, fuelling more efficiently the plasma core. Consequently, the density rises more at the centre than at the edge, so allowing the central line-averaged density to exceed $\bar{n}_G$, while the edge line-averaged density does not exceed $\bar{n}_{G_{edge}}$. A future quantitative analysis can tell us whether the change in the particle source alone can explain the peaking or a change in the transport properties should also be considered. In such a framework, the q-dependence of the density peaking at the disruption can also be easily explained. In fact, with increasing edge q, the connection length increases, thus creating more favourable conditions for the development of the MARFE. Neutral transport calculations are left to future work, so this discussion of neutral penetration should be considered as speculation. It is worth noting that MARFE has been observed in many machines, e.g. Alcator C [24], JET [25], ASDEX Upgrade [26] and TEXTOR [27], just before the density limit, and has been considered as the cause of the edge cooling that leads to the radiation collapse at the edge [9, 28]. In particular, in TEXTOR (a circular poloidal cross-section machine as FTU) non-disruptive discharges with a stationary density much higher than the Greenwald limit (up to a factor of 2.1) have been produced in L-mode after having suppressed the MARFE, by controlling the gap between the plasma and the limiter in the high-field side, without a sensible change in the peaking but with an increase in the thermal flux to the edge [27]. The situation in FTU seems to be different as MARFE does not lead directly to a disruption but can remain in a steady state for several energy confinement times, without degrading the bulk plasma confinement, and increasing the density profile peaking factor, at least in ohmic discharges in a highly clean plasma ($Z_{eff} < 1.5$) with a boron- or lithium-conditioned wall. To the best of our knowledge, this phenomenology has not been observed on other machines and has not been reported in the vast literature produced during the earliest experiments on MARFE, so that it is not easy to say whether or not it is a peculiarity of FTU. In particular, none of the previous publications has ever reported a systematic study of the effect of a strong MARFE activity on the density peaking. Note that the analysis of particle transport in discharges similar to those reported here, carried out by means of the gyrokinetic electromagnetic flux-tube code GKW [29], has shown that a possible additional mechanism for density peaking is an increase in the particle pinch due to the presence of light impurities [30]. The issue of core density and density peaking was addressed in a large number of previous experimental [31] and theoretical studies; in particular, different authors have previously shown a relationship between the density and the safety factor profiles, particularly in L-mode [32–36]. A more accurate analysis is needed to discuss the relation between the density peaking and the edge safety factor and to show whether the proposed explanations, namely the anomalous curvature pinch or the turbulent equipartition by trapped electrons, are consistent with the FTU data or not.

We have shown that the maximum achievable edge line-averaged density grows with the plasma current, according to the proposed *edge* Greenwald limit scaling, while the same scaling does not hold for the central line-averaged density due to density peaking effects: for example, for a fixed B_T, less peaked density profiles are typically produced at higher currents, thus masking the expected improvement of the density limit with input power in ohmically heated discharges (as expected on the basis of the *standard* Greenwald limit). In

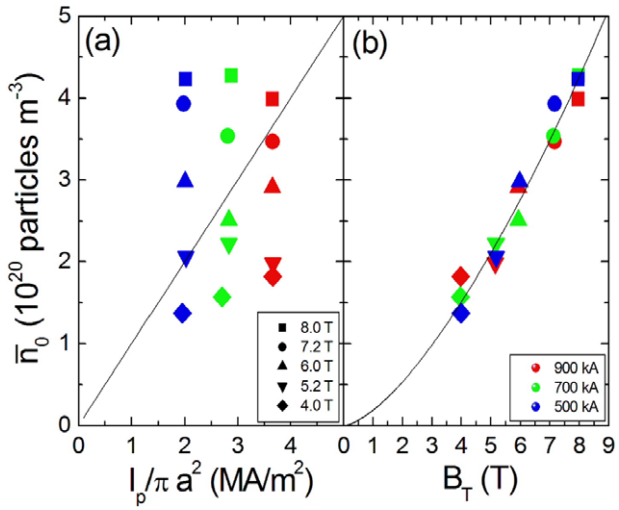

Figure 6. Central line-averaged density at the disruption for the density limit versus the plasma current density for different B_T (a) and versus B_T for different I_p values (b). See boxes in the figure for the meaning of symbols and colours. The solid lines correspond to the Greenwald density limit $\bar{n}_G$ (a) and to the new scaling law $\bar{n}_{new}$ (b).

figure 6, the central line-averaged density at the disruption for the density limit is shown as a function of the plasma current density for different B_T (a) and as a function of B_T for different plasma current densities (b). As we can see, the data show a substantial independence of the maximum achievable central line-averaged density on the average plasma current density, while we find a more than linear dependence on B_T: by doubling the value of B_T the value of the density limit is more than doubled. In particular, the best fit of the values of density corresponding to the disruption (expressed in units of 10^{20} particles m^{-3}) as a function of B_T (in T) is given by $\bar{n}_{new} = 0.19 \times B_T^{1.5\pm0.1}$, shown in the plot by a solid curve.

Various density limit scaling laws based on B_T have already been proposed in the literature. The first scaling law showing a dependence on B_T was the first absolute scaling of the density limit, the so-called *Murakami limit* [2]: the maximum central line-averaged density achieved by several machines appeared to scale as the ratio B_T/R, namely a weaker dependence on B_T than that observed on FTU. Actually, as the authors state [2], the *Murakami limit* was obtained on a set of discharges with the same edge safety factor ($q_a \simeq 5$), so it was impossible to discriminate between the dependence on I_p or B_T and the authors used this fact to claim the true limit dependent on the current (total input power). In the past, FTU has had the density limit not dependent on the plasma current [7], due to the fact that the plasma was contaminated by carbon and oxygen, but this limit was below the usual Greenwald one, and was extended injecting deuterium pellets into the plasma. In the present experiments, the plasma was clean and the Greenwald limit has been passed with gas puffing only. In 1982 Granetz [37] observed a density threshold for MHD activity in Alcator C with the threshold value increasing with the square of B_T and no dependence on I_p over a wide range of the edge safety factor. The observed MHD threshold does not represent a density limit, but the amplitude of the MHD activity increased rapidly above the MHD threshold until, at densities about 40% above the MHD threshold, a disruptive density limit was reached [4]. The scaling of the density threshold for MHD activity on FTU and its possible dependence on the toroidal magnetic field will be discussed in a future work. Referring to a circular poloidal cross-section machine such as FTU, the behaviour of the density limit with respect to the toroidal magnetic field was investigated on TEXTOR by varying B_T between 1.78 and 2.6 T and the density limit was found to be only marginally higher for lower B_T, leading to a scaling like $\bar{n}_{DL} \propto B_T^{-0.17}$ [27]. Also in divertor tokamaks various density limit scaling laws based on B_T have been proposed, e.g. the so-called 'BLS (Borrass, Lingertat, Schneider) scaling', where the scaling of the edge density at the disruption results from a model based on the analysis of the scrape-off layer region [38]. The model was extensively validated against ASDEX and JET data, showing, at fixed edge q, a square root dependence of the line-averaged density on the toroidal magnetic field [39]. Recently, the existence of a density limit in magnetized plasmas was proposed from first principles of electromagnetism, showing a dependence on the square of B_T [40]. It is worth mentioning that the new scaling law found for the density limit on FTU implies a favourable scaling for large values of B_T. For example, for a plasma current of 500 kA, according to the scaling law $\bar{n}_{new} = 0.19 \times B_T^{1.5}$, FTU is able to operate at central line-averaged densities up to 4.3×10^{20} particles m^{-3} (for $B_T = 8$ T), which is twice the value expected from the *standard* Greenwald scaling law $\bar{n}_G = I_p/\pi a^2$.

4. Conclusions

Density limit experiments performed on FTU indicate that in disruptions for the density limit the dependence of the density peaking on the edge safety factor, associated with the presence of a MARFE, plays a crucial role in the determination of a density limit scaling law when the central line-averaged density is considered. A new density limit scaling law results in which the central line-averaged density is solely dependent on the toroidal magnetic field. On the other hand, as a confirmation that the density limit is an edge limit, it is also found that a Greenwald-like scaling (i.e. depending on the current density) holds for the edge line-averaged density (at $r/a \simeq 4/5$). All of the above results are obtained in ohmically heated, gas fuelled, limited plasma discharges in L-mode in the presence of MARFEs. Future studies in FTU will analyse the behaviour of the density limit for lower values of toroidal magnetic field and plasma current as well as for plasmas in which the density peaking is produced by pellet injection or lithium-coated walls. It would be helpful to have also some discharges with additional heating for comparison with the literature, but both FTU auxiliary heating systems (LH and ECRH) have small effects at such high densities and most of the plasmas considered here would be centrally overdense for the 140 GHz frequency, preventing the ECH.

Acknowledgments

This work was supported by the Euratom Communities under the contract of Association between EURATOM-ENEA. The views and opinions expressed herein do not necessarily reflect those of the European Commission.

References

[1] Lawson J.D. 1957 *Proc. Phys. Soc.* B **70** 6
[2] Murakami M., Callen J.D. and Berry L.A. 1976 *Nucl. Fusion* **16** 347
[3] Stott P.E., Hugill J., Fielding S.J., McCracken G.M., Powell B.A. and Prentice R. 1977 *Proc. 8th European Conf. on Controlled Fusion and Plasma Physics (Prague, Czech Republic, 19–23 September 1977)* vol 1 p 37
[4] Greenwald M., Terry J.L., Wolfe S.M., Ejima S., Bell M.G., Kaye S.M. and Neilson G.H. 1988 *Nucl. Fusion* **28** 2199
[5] Stabler D. *et al* 1992 *Nucl. Fusion* **32** 1557
[6] Bell M.G. *et al* 1992 *Nucl. Fusion* **32** 1585
[7] Frigione D. *et al* 1996 *Nucl. Fusion* **36** 1489
[8] Maingi R. *et al* 1999 *J. Nucl. Mater.* **266** 598
[9] Greenwald M. 2002 *Plasma Phys. Control. Fusion* **44** R27–80
[10] Gormezano C., De Marco F., Mazzitelli G., Pizzuto A., Righetti G.B. and Romanelli F. 2004 *Fusion Sci. Technol.* **45** 297 www.new.ans.org/store/j_515
[11] Tudisco O. *et al* 2010 *Fusion Eng. Des.* **85** 902
[12] Mazzitelli G. *et al* 2011 *Nucl. Fusion* **51** 073006
[13] Lipschultz B. 1987 *J. Nucl. Mater.* **145** 15
[14] Canton A., Innocente P. and Tudisco O. 2006 *Appl. Opt.* **45** 9105
[15] Cenacchi G. and Taroni A. 1986 *Proc. 8th Computational Physics, Computing in Plasma Physics (Eibsee, Germany, 13–16 May 1986)* vol 10D (EPS) p 57
[16] De Angelis R. *et al* 1998 *Proc. 25th European Physical Society Conf. on Controlled Fusion and Plasma Physics (Prague, Czech Republic, 29 June–3 July 1998)* vol 1 p 1674
[17] Stabler A. *et al* 1989 *Proc. 16th European Conf. on Controlled Fusion and Plasma Physics (Venice, Italy, 13–17 March 1989)* vol 13B (part I) (ECA) p 23
[18] Kamada Y. *et al* 1991 *Nucl. Fusion* **31** 1827
[19] Fielding S.J. *et al* 1977 *Nucl. Fusion* **17** 1382
[20] Osborne T.H. *et al* 2001 *Phys. Plasmas* **8** 2017
[21] Messiaen A. *et al* 1996 *Phys. Rev. Lett.* **77** 2487
[22] Gao X. *et al* 2000 *Phys. Plasmas* **7** 2933
[23] Weynants R.R. *et al* 1999 *Nucl. Fusion* **39** 1637
[24] Lipschultz B. *et al* 1984 *Nucl. Fusion* **24** 977
[25] Wesson J.A. *et al* 1989 *Nucl. Fusion* **29** 641
[26] Mertens V. *et al* 1994 *Plasma Phys. Control. Fusion* **36** 1307
[27] Rapp J. *et al* 1999 *Nucl. Fusion* **39** 765
[28] Shuller F.C. 1995 *Plasma Phys. Control. Fusion* **37** A135
[29] Peeters A. *et al* 2009 *Comput. Phys. Commun.* **180** 2650
[30] Romanelli M. *et al* 2011 *Nucl. Fusion* **51** 103008
[31] Weisen H. *et al* 2004 *Plasma Phys. Control. Fusion* **46** 751
[32] Yankov V.V. 1994 *JETP Lett.* **60** 171 www.jetpletters.ac.ru/ps/1323/article_20003.shtml
[33] Nycander J. and Yankov V.V. 1995 *Phys. Plasmas* **2** 2874
[34] Isichenko M.B., Gruzinov A.V. and Diamond P.H. 1995 *Phys. Rev. Lett.* **74** 4436
[35] Baker D.R. 1997 *Phys. Plasmas* **4** 2229
[36] Angioni C. *et al* 2003 *Phys. Rev. Lett.* **90** 205003
[37] Granetz R.S. 1982 *Phys. Rev. Lett.* **49** 658
[38] Borrass K., Lingertat J. and Schneider R. 1998 *Contrib. Plasma Phys.* **38** 130
[39] Borrass K. *et al* 2004 *Nucl. Fusion* **44** 752
[40] Carati A., Zuin M., Maiocchi A., Marino M., Martines E. and Galgani L. 2012 *Chaos* **22** 033124